Conference on Modelling Fluid Flow (CMFF'12)
The 15th International Conference on Fluid Flow Technologies
Budapest, Hungary, September 4-7, 2012

DETAILED COMPARISON OF NUMERICAL FLOW PREDICTIONS IN CEREBRAL ANEURYSMS USING DIFFERENT CFD SOFTWARE

Philipp BERG[1], Gábor JANIGA[1], Dominique THÉVENIN[1]

[1] Department of Fluid Dynamics and Technical Flows, University of Magdeburg. Universitaetsplatz 2, D-39106 Magdeburg, Germany. Tel.: +49 391 67 181 95, Fax: +49 391 67 128 40, E-mail: berg@ovgu.de

ABSTRACT

Within the last decades, Computational Fluid Dynamics (CFD) simulations became increasingly important to investigate flow phenomena that are difficult to analyze experimentally. In the field of medical engineering, for instance concerning blood flows in cerebral aneurysms, computer-based approaches could open up new opportunities to support medical practitioners before high-risk interventions.
The present work compares commercial and open-source CFD software packages in order to determine their reliability for predicting medical blood flows. The haemodynamic simulations were carried out on unstructured as well as block-structured grids of a patient-specific geometry. Blood is treated as an incompressible, isothermal and Newtonian fluid. To provide a realistic inflow condition a time- and space-dependent Womersley velocity profile is implemented.
Several comparisons found that if the geometric complexity allows block-structured mesh generation, hexahedral grids should be preferred in order to predict the blood flow. Steady and unsteady simulations resulted in almost equal parameters for velocity and wall shear stresses at peak pressure. Nevertheless, unsteady flow patterns that may cause remodelling processes of the arterial walls, can only be analysed with unsteady assumptions. Finally, it can be stated that OpenFOAM® is a comparable CFD tool regarding haemodynamic simulations in cerebral aneurysms.

Keywords: cerebral aneurysm, CFD, Fluent, haemodynamics, OpenFOAM

NOMENCLATURE

A	$[m^2]$	surface area
C	$[-]$	Fourier coefficient
f	$[1/s]$	frequency
ICI	$[-]$	inflow concentration index
N	$[-]$	number of elements
P	$[-]$	number of processors
Q	$[m^3/s]$	flow rate
R	$[m]$	mean vessel radius
r	$[m]$	radial coordinate
T	$[s]$	period of the cardiac cycle
TOT	$[s]$	turnover time
t	$[s]$	time
$\underline{U}$	$[m/s]$	absolute velocity vector
w	$[m/s]$	axial velocity component
α	$[-]$	Womersley number
η	$[Pa \cdot s]$	dynamic viscosity
κ	$[-]$	rate of change
ν	$[m^2/s]$	kinematic viscosity
ρ	$[kg/m^3]$	density
Φ	$[-]$	variable
τ	$[Pa]$	wall shear stress
ω	$[1/s]$	angular frequency

Subscripts and Superscripts

A	aneurysm
in	flow direction into the aneurysm
inlet	inflow of the flow domain
k	count index of the Fourier series
max	maximum value
mean	mean value
n	count index of the rate of change
o	ostium

1. INTRODUCTION

In order to investigate highly complex problems Computational Fluid dynamics (CFD) evolved to a sophisticated method to approach the behaviour of flow phenomena and their effects on key parameters. Within the last decades, several advantages were found in contrast to experimental procedures. For instance, numerical methods may be able to consider scales, which cannot be captured experimentally so far. In many cases, high performance computing hardware is less expensive than complex measuring equipment. Additionally, a better reproducibility can be achieved due to a lower systematic error and to a lower influence

of varying process conditions.
These advantages are useful in the field of medical engineering, for instance concerning blood flow in cerebral aneurysms. These are abnormal focal dilatations of weakened arterial walls resulting from a process of remodelling and growing [1]. Without treating or with a wrong treatment an enhanced risk of rupture exists, with rupture leading to heavy disabilities or even a sudden death [2]. Therefore, specific research regarding haemodynamics in cerebral aneurysms is essential. Qualitative observations as well as time-dependent measurements of the velocity components are possible by means of 7-Tesla-Magnetic Resonance Tomography (MRT) [3]. However, investigating the pressure distribution along certain vessel regions or the change of wall shear stresses within a cardiac cycle can only be achieved numerically.
Recent works show that computational techniques are promising in simulating the blood flow in the cerebral aneurysm itself and also the influence on the haemodynamics after treatments like *Coiling* or *Stenting* [4, 5]. Validation of the numerical results by means of digital subtraction angiography (DSA) has been carried out successfully as well [6].
Although those computer-based approaches could open up new opportunities to support medical practitioners before high-risk interventions, even published results should always be questioned critically. Sforza et al. [7] investigated the haemodynamics in intracranial aneurysms in order to identify flow patterns influencing aneurysm progression. After their computations and in vivo observations they found that numerical models tend to be oversimplified and do not reproduce accurately the complex flow structure.
In order to obtain predictions within hours, most numerical simulations rely on numerous assumptions and model reductions, depending on the desired accuracy. Therefore, individual conditions as well as all complex biological regulation mechanisms controlling the human vascular system cannot be considered in standard algorithms at the state of the art. Due to this circumstance, the acceptance of CFD in medicine is still limited in practice, leading to controverse discussions, e.g., regarding the pressure prediction in cerebral aneurysms after treatment with flow diverting devices [8]. Also the wide range of modelled and measured boundary conditions compared in [9] shows reliable computational predictions remain highly challenging.
However, various software packages or in-house algorithms are used and the number of computations considering medical flows increased rapidly over the past years. Those tools are either commercial or contributed through an open-source license. In order to determine their reliability for predicting medical blood flows one of the leading products of each category is chosen and compared afterwards. The commercial CFD solver ANSYS Fluent® as well as the open-source code OpenFOAM® are used to investigate the haemodynamics in a patient-specific cerebral aneurysm. The computations are based on a reconstructed aneurysm geometry measured by means of Magnetic Resonance Imaging (MRI). Both packages use a finite volume method whereby steady as well as unsteady simulations have been carried out to analyse the influence of spatial discretisation. Furthermore, important parameters like accuracy, computational costs, parallel efficiency, problem-specific model extension and user-friendly interfaces are assessed. Finally, conclusions are drawn to highlight strengths and weaknesses of the individual software packages and more generally concerning CFD for haemodynamics.

2. MATERIALS AND METHODS

The following sections demonstrate how the present CFD simulations were set up based on raw patient-specific imaging data. Spatial and temporal discretisation methods as well as post-processing are described in detail.

2.1. Vascular Model

In order to perform the desired blood flow simulations it is necessary to generate a suitable geometry model. Several techniques exist to obtain three-dimensional data of cerebral arteries by means of imaging systems. For instance CTA (Computed Tomography Angiography) scans as well as MRI scans use contrast agents to visualise the blood and therefore the boundaries of the surrounding vessel walls.
The present geometry was obtained by using a DSA, commonly utilized during an operation. The resulting projection consists of two-dimensional data in the first place but a 3D reconstruction is possible when connecting multiple datasets achieved by rotating the C-arm around the patient. At present, such a 3D Rotational Angiography (3DRA) provides the highest local resolution and can be seen as the gold standard in terms of imaging methods. The segmentation of the aneurysm geometry was performed using a seeded region-growth algorithm. Optical artefacts occurring during the imaging process have been eliminated as well. To achieve a high surface quality the segmentation results were transformed into discrete meshes and smoothed afterwards [10].
The resulting cerebral aneurysm was located on the middle cerebral artery (MCA) connected to the circle of Willis, which supplies blood to the brain and ensures an unhindered blood flow into the important parts. Figure (1) presents the shape of the investigated geometry from different points of view. The inflow region is positioned at the bottom and two outlets can be detected on the top.

To identify the influence of the mesh density on several parameters, five unstructured grids were generated with a number of elements ranging from circa 230.000 to 12.5 millions. For the

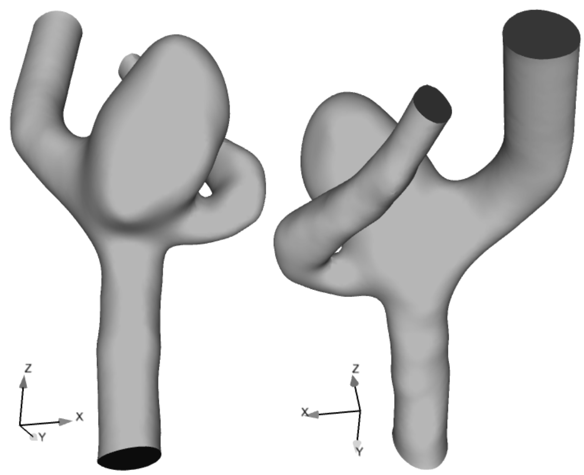

Figure 1: Patient-specific geometry of the investigated cerebral aneurysm

spatial discretisation the commercial meshing software ANSYS ICEM-CFD ® 13.0 (Ansys Inc., Canonsburg, PA, USA) was used. A Delaunay method created the tetrahedral elements with a maximum size ranging from 0.2 to 0.05 mm. Due to the element flexibility even complicated geometries like patient-specific aneurysms are able to be meshed within a short time. In areas of strong changes in geometric direction, especially in the region between the aneurysm sack and the vessel branches local refinements of the meshes were carried out. Therefore, flow patterns are better resolved in these zones. Additionally, three boundary layers of prismatic elements were inserted to ensure a finer resolution close to the vessel wall. Their initial height ranges from 40 to 15 μm and a growth ratio of 1.3 was defined. Corresponding to the previously described meshes presented in Table (1) another five unstructured meshes were generated without boundary layers. Therefore, the necessity of such layers in blood flow simulations can be investigated.

Table 1: Number of elements corresponding to the unstructured meshes without and with prismatic layers at the walls

Mesh number	Number of elem. (without prisms)	Number of elem. (with prisms)
1	228.317	256.723
2	516.230	551.612
3	1.678.508	1.667.308
4	3.142.530	3.016.046
5	12.468.478	12.274.395

To compare results obtained on structured and unstructured grids, another (block-structured) grid was generated consisting of 1.7 million hexahedral elements. The cell growth ratio from the walls to the inner volume was chosen similar to the unstructured one. Figure (2) shows an unstructured mesh with boundary layers (top) and the structured grid (bottom), respectively.

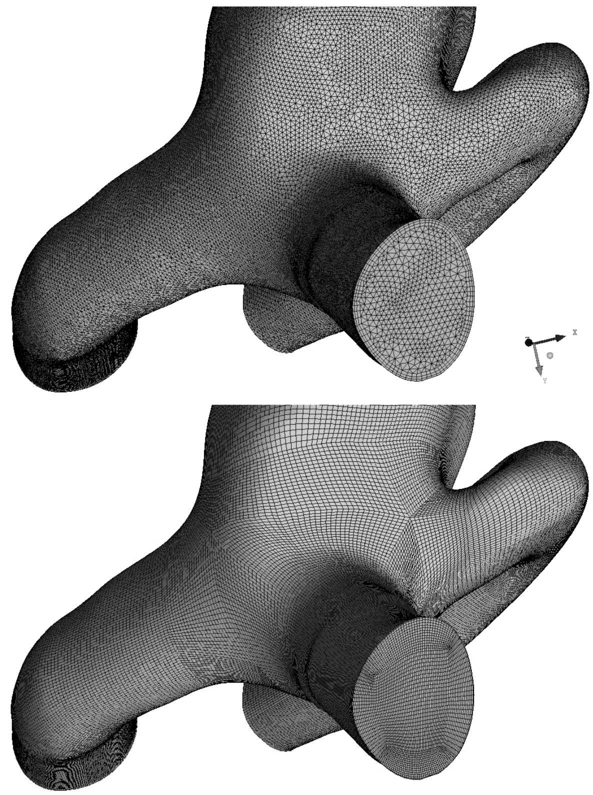

Figure 2: Presentation of unstructured mesh # 3 with boundary layers (top) and the structured mesh (bottom)

2.2. Haemodynamic simulation

Based on the generated meshes steady as well as unsteady haemodynamic simulations were carried out. In all cases blood is treated as an isothermal, incompressible ($\rho = 1055 \frac{kg}{m^3}$) and Newtonian fluid with a constant dynamic viscosity $\eta = 4.265 \cdot 10^{-3}\ Pa \cdot s$ [11]. Indeed, blood as a suspension of plasma and cellular components shows non-Newtonian behaviour especially at low shear stresses. Previous computations have shown that considering the viscosity dependency with the commonly used *Carreau-Yasuda*-model does not lead to any noticeable differences in the velocity profiles due to the large arterial diameters [12].

Fully developed Womersley velocity profiles are implemented as inflow boundary conditions [13]. In contrast to common parabolic velocity profiles this time- and location-dependent solution considers the pulsatile character of the blood flow. Hence, this analytical approach shows a good agreement with measurements. As given in Eq. (1) the axial velocity component $w(r,t)$ is composed of a steady and an oscillatory part [14] and affected by the mean vessel radius R, the Bessel functions J_0 and J_1 of the first kind (of order 0 and 1), and the Womersley number α. This dimensionless number characterises the ratio of unsteady acceleration forces to frictional forces (see Eq. (2)) with the angular frequency $\omega = 2\pi f$ and the kinematic viscosity $\nu = \eta/\rho$. With respect to the present study a Womersley number $\alpha = 3.13$ was calculated.

$$w(r,t) = \frac{2C_0}{\pi R^2}\left[1-\left(\frac{r}{R}\right)^2\right] + \sum_{k=1}^{N}\left\{\frac{C_k}{\pi R^2}\left[\frac{1-\frac{J_0\left(\alpha_k \frac{r}{R} i^{3/2}\right)}{J_0\left(\alpha_k i^{3/2}\right)}}{1-\frac{2J_1\left(\alpha_k i^{3/2}\right)}{\alpha_k i^{3/2} J_0\left(\alpha_k i^{3/2}\right)}}\right]\right\} e^{ik\omega t} \tag{1}$$

$$\alpha_k = R\sqrt{\frac{k\cdot\omega}{\nu}} \tag{2}$$

The corresponding synthetically generated flow rate for one cardiac cycle is described by a set of complex Fourier coefficients C_k and presented in Figure (3). The arterial walls are assumed to be rigid and a no-slip boundary condition is defined forcing the velocity component to be zero [15]. Due to a lack of knowledge regarding the pressure variation in the different vessel branches a traction-free condition is imposed at the outlets of the domain.

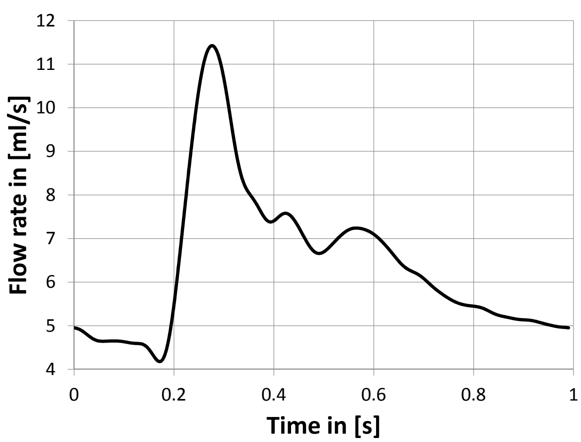

Figure 3: Flow rate for one cardiac cycle (T=0.99 s) corresponding to the inflow boundary condition of unsteady simulations

The governing Navier-Stokes equations were solved using the commercial software package ANSYS Fluent® 13.0 and the open-source code SGI OpenFOAM® 2.0.1 (SGI Inc., Fremont, CA, USA), respectively. Both are based on a finite volume method approximating the integral form of these governing equations. For the steady cases a semi-implicit coupling algorithm (SIMPLE) was used to iteratively calculate the pressure and velocity fields. Convergence was obtained when the scaled residuals of pressure and momentum decreased below a value of 10^{-5}. The time-dependent simulations were carried out with a pressure-implicit algorithm (PISO) executing 2 steps of pressure correction within each loop. A constant time step size was chosen as 10^{-3} s according to the stability condition (Courant number ≤ 1), which was estimated in advance. Within each time step scaled residuals of 10^{-4} were demanded. Only the second cardiac cycle was analysed, discarding the first cycle [16].
Due to the high number of element the computational domain has been decomposed in advance in order to simulate in parallel. The Scotch-method was used as a decomposition algorithm leading to domains with equivalent element numbers [17]. All simulations were carried out on the in-house cluster Kármán consisting of 544 computing cores (AMD Quad Core 2.1 GHz) and an InfiniBand network.

2.3. *Analysis*

The effect of mesh type and resolution on several variables was first investigated. Therefore, in Eq. (3) a rate of change κ was defined describing how a certain averaged parameter Φ changes depending on the number of elements N. A multiplication with 10^8 adjusts κ to a manageable order of magnitude.

$$\kappa_n = \left|\frac{\Phi_{n+1}-\Phi_n}{N_{n+1}-N_n}\right| \cdot 10^8 \quad n = 1\dots 4 \tag{3}$$

In the scope of this study, the maximum velocity U_{max}, its temporal mean value U_{mean} as well as the mean wall shear stress τ_{mean} were analysed. Additionally, in Eqs. (4) to (5) different criteria commonly used in haemodynamic post-processing were implemented based on the calculated velocity fields. The turnover time (TOT), which is defined by the ratio of the aneurysm volume V_A to the flow rate entering the aneurysm Q_{in} describes how long the blood resides within the sack [12]. Q_{in} is computed using the entering velocity times the inflow area A_{in}, which is part of the total ostium area A_o (area between the aneurysm and the corresponding vessel). The entering blood can be expressed as well by the inflow concentration index (ICI) [18]. Compared to TOT, ICI involves also the flow rate at the inlet of the cerebral artery Q_{inlet}.

$$TOT = \frac{V_A}{Q_{in}} \tag{4}$$

$$ICI = \frac{Q_{in}/Q_{inlet}}{A_{in}/A_o} \tag{5}$$

Post-processing was accomplished with EnSight® 9.2 (CEI Inc., Apex, NC, USA) and

Kitware ParaView® 3.10.1 (Kitware, Inc., Clifton Park, NY, USA).

3. RESULTS

After carrying out the previously described simulations and analyses it is now possible to compare 1) the meshing strategy, 2) the choice of the solver and 3) the importance of temporal variations. Figures (4) to (5) present an exemplary velocity field as well as the corresponding streamlines for a steady case.

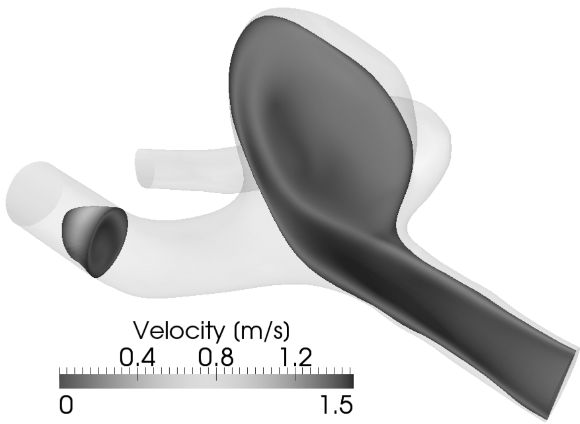

Figure 4: Exemplary velocity distribution within the flow domain based on a block structured mesh

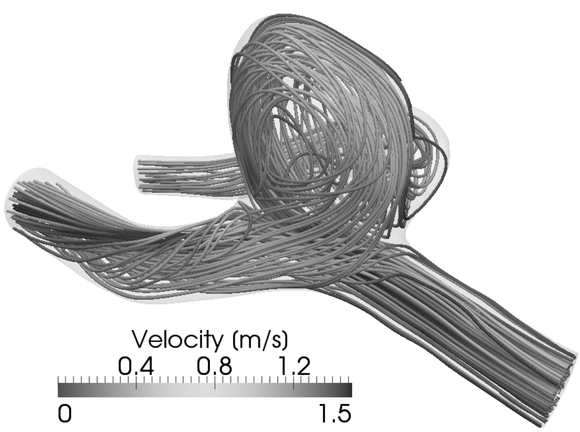

Figure 5: Streamlines corresponding to the velocity field of a block structured simulation

These figures reveal that the flow enters the aneurysm at its bottom and remains close to the aneurysmal wall until it exits sideways back to the arterial branches. Afterwards, approximately 77 % of the mass flow rate remain within the frontal vessel and 23 % leave through the smaller one, respectively. Due to the geometric situation a helical flow pattern develops in the branches resulting in non-parabolic velocity profiles.

3.1. Unstructured vs. Structured

To quantitatively compare the different meshing technologies two variables were derived from steady Fluent® simulations. The spatially averaged velocities U_{mean} as well as the mean wall shear stress τ_{mean} of the unstructured meshes are presented in Table (2) and (3) with their rates of change κ.

With increasing number of elements κ decreases in all cases and indicates only minor variations between the last two considered mesh densities. Comparing unstructured based simulations with and without layers directly, negligible differences appear between U_{mean} (0.17 % - 0.81 %). In contrast, higher deviations occur with respect to τ_{mean} ranging from 11 % to 19.7 %. Considering the resulting values of the block-structured simulation an average velocity of $0.704\ \frac{m}{s}$ and a mean wall shear stress of $29.68\ Pa$ was found which is in good agreement with the results achieved by unstructured meshes with prisms. This shows that the use of boundary layers is highly recommended when analyses regarding the vessel walls are of interest.

Table 2: Rate of change for the unstructured meshes without layers

Nr.	U_{mean} in $[\frac{m}{s}]$	κ in $[\frac{m}{s}]$	τ_{mean} in $[Pa]$	κ in $[Pa]$
1	0.6598	5.4483	35.5745	164.943
2	0.6702	0.9926	35.0995	58.6467
3	0.6814	0.3063	34.4356	28.0244
4	0.6859	0.0572	34.0169	9.11
5	0.6913	-	33.1672	-

Table 3: Rate of change for the unstructured meshes with layers

Nr.	U_{mean} in $[\frac{m}{s}]$	κ in $[\frac{m}{s}]$	τ_{mean} in $[Pa]$	κ in $[Pa]$
1	0.6639	3.9859	28.5623	81.5409
2	0.6756	0.6206	28.8028	32.5714
3	0.6825	0.4131	29.1662	3.8082
4	0.6881	0.0613	29.2176	3.2668
5	0.6939	-	29.52	-

The analyses of additional parameters e.g. regarding pressure distribution or regions of elevated wall shear stresses showed the same tendencies. Hence, it can be concluded for unstructured meshes that the largest changes occur at element numbers smaller than approximately 3 millions. The differences between 3 and 12 million cells are relatively small and the values are closest to those of the block structured mesh. This finding supports the assumption that an increased effort during mesh generation allows to achieve more accurate results within shorter computational times.

3.2. Fluent vs. OpenFOAM

After identifying the impact of spatial discretisation on several parameters, a comparison of two CFD packages followed. At first the mean velocity of steady computations was investigated and a good agreement between both solvers can be observed. The deviation ranges from 0.12 % at the coarsest mesh density to 0.34 % for mesh # 5. However, the introduced variables TOT and ICI reveal larger differences. The predicted turnover times deviate between 1.4 and 5.8 %. Approximately equal variations occur for the inflow concentration indices ICI (1.3 - 7.1 %).

In addition to the flow variables, the required simulation time using different numbers of processors was assessed. In all cases, Fluent® was faster in reaching the demanded residuals of 10^{-5}. Due to license restrictions with Fluent® only up to 8 cores were considered. While there is no problem for parallelisation with OpenFOAM®, the usage of more processing units leads to a higher communication among the slaves, rapidly decreasing efficiency. In this context, it is always important to analyse the speed-up factor and the parallel efficiency, respectively. Figure (6) shows the corresponding results.

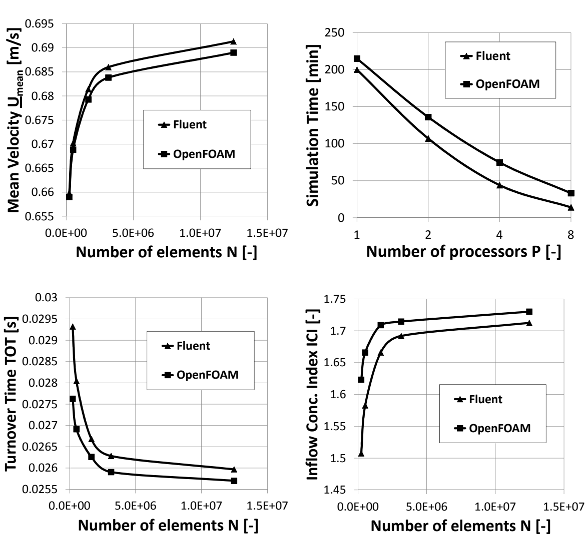

Figure 6: Comparison between ANSYS Fluent® and OpenFOAM®: Mean velocity (top left), simulation time as function of the number of processors for case # 2 (top right), turnover time (bottom left), inflow concentration index (bottom right)

Overall, OpenFOAM® as a freely available open-source software package constitutes a valuable and cost-efficient alternative to Fluent® in order to predict haemodynamics in cerebral aneurysms.

3.3. Steady vs. Unsteady

The mean velocity of the time-depended simulation was temporally averaged over one cardiac cycle and compared to U_{mean} of the steady solution. Only minor differences ($\leq$ 5 %) were noticeable. The same tendencies appear regarding the maximum velocity and the wall shear stresses presented in Figure (7). Elevated regions are predicted in both cases at the transition of vessel and aneurysm and in areas of strong changes in geometric direction. The largest visible differences between both cases occur on the walls of the branches.

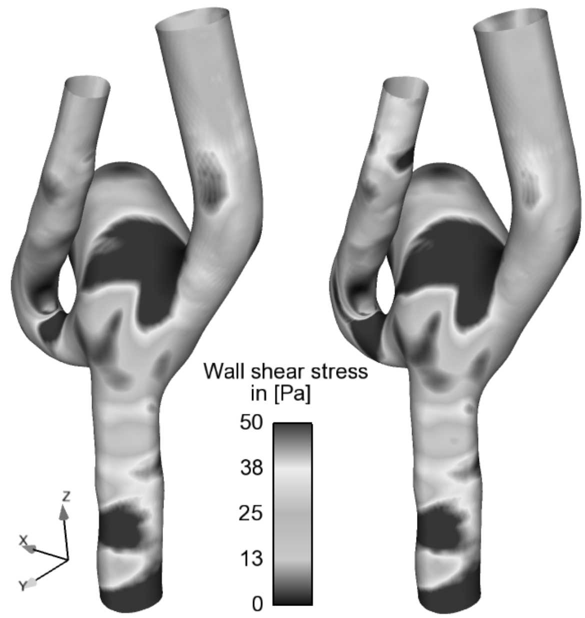

Figure 7: Steady wall shear stress (left) compared to the temporal average of the unsteady simulation (right)

Hence, time-consuming unsteady simulations might be be replaced by steady assumptions when only average information is of interest. However, in order to analyse time-dependent flow patterns, which may be responsible for vessel wall remodelling, unsteady simulations obviously need to be performed. One such example would be the existence of an oscillating flow near the aneurysm dome.

4. CONCLUSION

Firstly, the comparison between unstructured and block structured meshing methodologies shows that significant differences occur depending on the mesh resolution. Although mesh generation of unstructured grids is clearly less time-consuming, a higher resolution is necessary to achieve comparable accuracy. This leads to larger simulation times due to the high number of elements and to a slower convergence by contrast with structured meshes. Hence, higher computational costs will result. If possible, the generation of hexahedral grids is recommended. If vessel parameters like the wall shear stress or its gradients are needed and a block-structured meshing is too complex, prism layers are essential at the boundaries.

Secondly, it was found that the results achieved by the open-source CFD software OpenFOAM® were in a good agreement with that of Fluent ®, which was only minimally higher in all cases. Although simulation times of OpenFOAM® were slightly higher in order to achieve a converged state, parallelisation is possible with OpenFOAM® without any license restriction. This could be an important factor for an application in clinical workflows where reliable results are often required rapidly before decision-making. In terms of user-friendliness and getting familiar with the necessary steps to set up haemodynamic simulations Fluent® is far more intuitive in particular due to its graphical user interface (GUI). After a reference case has been set up, both software packages are able to derive simulations very quickly and without GUI for instance using a journal file.

The analysis of averaged parameters like the mean velocity or wall shear stresses revealed no major differences between steady and unsteady simulations. Hence, steady simulations may be used to estimate such quantities. In order to investigate fluctuating flow patterns, which may influence the wall properties, time-dependent computations are obviously required.

Overall it can be stated that OpenFOAM® is a competitive CFD tool regarding haemodynamic simulations in cerebral aneurysms. Furthermore, it is worth putting additional effort in the generation of block-structured meshes to achieve afterwards more accurate and stable steady and unsteady simulations. Further investigations aim onto the experimental validation of numerical results. Here, four-dimensional (time dependent velocity vectors) measurements using a 7-Tesla-MRT or Particle Tracking Velocimetry techniques are suitable [19].

ACKNOWLEDGEMENTS

The authors like to express their gratitude to Dr. Oliver Beuing for providing the patient-specific MRT data of the cerebral aneurysm. Special thank also goes to Dipl.-Ing. Mathias Neugebauer who supported the investigations by reconstructing the patient data in order to generate a geometric model.

References

[1] Lasheras, J. (2007) The biomechanics of arterial aneurysms. *Annual Review of Fluid Mechanics*, **39**, 293–319.

[2] Payner, T., Melamed, I., Ansari, S., Leipzig, T., Scott, J., DeNardo, A., Horner, T., Redelman, K., and Cohen-Gadol, A. (2011) Trends over time in the management of 2253 patients with cerebral aneurysms: A single practice experience. *Surgical Neurology International*, **2**, 110–115.

[3] Gasteiger, R., Janiga, G., Stucht, D., Hennemuth, A., Friman, O., Speck, O., Markl, M., and Preim, B. (2011) *Bildverarbeitung für die Medizin 2011*, chap. Vergleich zwischen 7 Tesla 4D PC-MRI-Flussmessung und CFD-Simulation, pp. 304–308. Springer, Berlin Heidelberg New York.

[4] Mitsos, A., Kakalis, N., Ventikos, Y., and Byrne, J. (2008) Haemodynamic simulation of aneurysm coiling in an anatomically accurate computational fluid dynamics model: technical note. *Neuroradiology*, **50**, 341–347.

[5] Ugron, Á., Szikora, I., and Paál, G. (2012) Computer simulation of intracranial aneurysm treatment using densely woven stents. *Proc. 5th European Conference of the International Federation for Medical and Biological Engineering*, pp. 442–445.

[6] Ho, H., Wu, J., and Hunter, P. (2011) *Computational Biomechanics for Medicine*, chap. Blood Flow Simulation in a Giant Intracranial Aneurysm and Its Validation by Digital Subtraction Angiography, pp. 15–26. Springer, Berlin Heidelberg New York.

[7] Sforza, D., Putman, C., and Cebral, J. (2009) Hemodynamics of cerebral aneurysms. *Annual Review of Fluid Mechanics*, **41**, 91–107.

[8] Cebral, J., Mut, F., Raschi, M., Scrivano, E., Ceratto, R., Lylyk, P., and Putman, C. (2011) Aneurysm rupture following treatment with flow-diverting stents: Computational hemodynamics analysis of treatment. *American Journal of Neuroradiology*, **32**, 27–33.

[9] Marzo, A., et al. (2011) Computational hemodynamics in cerebral aneurysms: The effects of modeled versus measured boundary conditions. *Annals of Biomedical Engineering*, **39**, 884–896.

[10] Neugebauer, M., Janiga, G., Beuing, O., Skalej, M., and Preim, B. (2010) Computer-aided modelling of blood flow for the treatment of cerebral aneurysms. *International Journal of Biomedical Engineering and Technology*, **55**, 37–41.

[11] Thews, G., Schmidt, R., and Lang, F. (2000) *Physiologie des Menschen*. Springer, Berlin Heidelberg New York.

[12] Berg, P., Janiga, G., and Thévenin, D. (2011) Investigation of the unsteady blood flow in cerebral aneurysms with stent using the open-source software openfoam. *Proc. Open Source CFD International Conference*.

[13] Womersley, J. (1955) Method for the calculation of velocity, rate of flow and viscous drag in

arteries when the pressure gradient is known. *American Journal of Physiology*, **127**, 553–563.

[14] Nichols, W. and O'Rourke, M. (2005) *McDonald's Blood Flow In Arteries*. Hodder Arnold.

[15] Anor, T., Grinberg, L., Baek, H., Madsen, J., Jayaraman, M., and Karniadakis, G. (2010) Modeling of blood flow in arterial trees. *Systems Biology and Medicine*, **2**, 612–623.

[16] Castro, M., Putman, C., and Cebral, J. (2008) *Computational Hemodynamics of Cerebral Aneurysms - Assessing the Risk of Rupture from Hemodynamic Patterns*. VDM Verlag Dr. Mller, Saarbrcken.

[17] Pellegrini, F. and Roman, J. (1996) Scotch: A software package for static mapping by dual recursive bipartitioning of process and architecture graphs. *Proc. HPCN'96, Brussels, Belgium*.

[18] Cebral, J., Mut, F., Weir, J., and Putman, C. (2011) Quantitative characterization of the hemodynamic environment in ruptured and unruptured brain aneurysms. *American Journal of Neuroradiology*, **32**, 145–151.

[19] Bendicks, C., Tarlet, D., Roloff, C., Bordás, R., Wunderlich, B., Michaelis, B., and Thévenin, D. (2011) Improved 3-d particle tracking velocimetry with colored particles. *Journal of Signal and Information Processing*, **2**, 59–71.